Applied Energy 168 (2016) 179–192

Contents lists available at ScienceDirect

Applied Energy

journal homepage: www.elsevier.com/locate/apenergy

A bi-layer optimization based temporal and spatial scheduling for large-scale electric vehicles

Lifu He [a,c], Jun Yang [a,*], Jun Yan [b], Yufei Tang [b], Haibo He [b]

[a] School of Electrical Engineering, Wuhan University, Wuhan 430072, PR China
[b] Department of Electrical, Computer, and Biomedical Engineering, University of Rhode Island, RI 02881, United States
[c] State Grid Hunan Electric Power Company Disaster Prevention and Reduction Center, Changsha 410129, PR China

HIGHLIGHTS

- A bi-layer scheme is proposed to optimize EVs charging and discharging behavior.
- The charging loads allocation in both temporal and spatial domain is optimized.
- Both the transmission system level and distribution system level are considered.
- The uncertainty and volatility of wind power are considered by using the scenarios.
- Method to evaluate the performance of proposed scheme is elaborated and demonstrated.

ARTICLE INFO

Article history:
Received 5 May 2015
Received in revised form 9 December 2015
Accepted 24 January 2016
Available online 8 February 2016

Keywords:
Unit commitment
Electric vehicle
Bi-layer optimization
Charging and discharging scheduling
Wind power
PM2.5 emissions

ABSTRACT

Electric vehicle (EV) is a promising, environmental friendly technique for its potential to reduce the using of fossil fuels. Massive EVs pose both opportunities and challenges for power systems, especially with the growing amount of wind-power integration. This paper investigates the problem of collaborative optimization scheduling of generators, EVs and wind power. A novel bi-layer optimization of transmission and distribution system is proposed to solve the scheduling problem of EVs charging and discharging load from respective time and space domain in the presence of wind-power. The upper layer optimization in transmission grid coordinates EVs with thermal generators, base load, with the consideration of wind power, to optimize load periods of EVs in the time domain. The lower layer optimization in distribution grid then spatially schedules the location of EVs load. Based on a power system benchmark with a 10-unit transmission grid and an IEEE 33-bus distribution grid, the performance of the proposed bi-layer optimization strategy is evaluated. The impacts of electricity price profile, EVs penetration and EVs load location are analyzed. Simulation results show that the proposed bi-layer optimization strategy can accommodate wind power and improve both the economics of grid operation and benefits of EV users by scheduling EVs charging and discharging temporally and spatially. Also, the results have shown that the location of EVs charging and discharging load is critical for the distribution network planning.

1. Introduction

Fossil fuel shortages and environmental protection have raised concerns in economic development. Large-scale deployment of electric vehicles (EVs) could be a potential solution to reduce the dependence on fossil fuel and protect the environment, and many countries and automobile manufacturers are making great efforts to promote the use of electric vehicles [1,2]. EVs are often represented by distributed and mobile power demands in power system; their distributed storage ability is also available to the power grid [3]. Using Vehicle to Grid (V2G) technology, EVs can help shift the peak load and reduce operating cost and emission of generators by optimal charging and discharging [4]. In the meantime, uncoordinated charging or discharging of a large number of EVs may lead to some problems in power grid, such as power congestion, under-voltage, grid instability, power quality, relay, frequency and other power grid problems [5–9].

Wind power is a clean and renewable energy that has been widely installed in power systems. However, due to the nature of

* Corresponding author at: School of Electrical Engineering, Wuhan University, Luo-jia-shan, Wuchang District, Wuhan City, Hubei 430072, PR China. Tel.: +86 13995638969.
E-mail address: JYang@whu.edu.cn (J. Yang).

http://dx.doi.org/10.1016/j.apenergy.2016.01.089
0306-2619/

wind power with uncertainty and fluctuation, it is difficult to be predicted accurately. As a result, wind power brings new challenges to the operation of power grid. As distributed and mobile energy storage units, EVs can smooth the fluctuation of wind power through charging and discharging guided by smart electricity price. Therefore, to improve both wind power accommodation ability and economical efficiency of power grid operation, there is potential benefits to develop the optimal scheduling strategy of power grid with the consideration of wind power and charging and discharging behavior of massive EVs.

EVs are connected to the distribution network of power grids and related problems have been well studied. Literature [10] employed the linear programming to determine the optimal charging rate for each EV to avoid excessive voltage drops and overloading of network components in distribution system. Literature [11] proposed a EVs charging and discharging strategy based on optimal power flow (OPF) solved by improved particle swarm optimization (PSO). Although this method is capable of coordinating EVs charging and discharging in distribution network, it omitted the power supply constraints from the transmission network. Literature [12] explored the relationship between feeder losses, load factor, and load variance in the context of coordinated EV charging in distribution network. It verified that these relationships approximately hold independent of system topology, and computation time and problem convexity can be reduced using load factor or load variance as the objective function. In Literature [13], an optimal scheduling model was proposed for large number of EVs parked in an urban parking lot. And some practical constraints including desired charging electricity price, remaining battery capacity, remaining charging time and age of the battery were considered in the proposed model. An event-triggered scheduling scheme for V2G based on the scenario of stochastic PEV connection to smart grid was proposed in Literature [14]. In Literature [15], to promise higher income for sub-aggregators and less energy not charged for vehicles while ensuring the convenience for residents, the presented model facilitated the participation of sub-aggregators in the aggregation of electric vehicles in a residential complex including a smart building and a smart parking lot. Literature [16] discussed the smart charging of electric vehicles with photovoltaic power and vehicle-to-grid technology in a microgrid. Literature [17] developed a smart charging framework to identify the benefits of non-residential EV charging to the load aggregators and the distribution grid. Literature [18] presented an optimization method that focuses on controlling the rate at which EVs charge over a 24-h time horizon. Literature [19] proposed a local control scheme whereby individual electric vehicle charging units attempt to maximize their own charging rate while maintaining local network conditions within acceptable limits. Literature [20] demonstrated the potential benefits and impacts of unidirectional V2G. In literature [21], a dispatch algorithm for EVs performing unidirectional regulation was developed. Literature [22] demonstrated the potential benefits and impacts of combining the bids of regulation and responsive reserves of unidirectional V2G. Literature [23] proposed a voltage feedback controller for EV charging. In literature [24], an optimal bidding of ancillary services coordinated across different markets was proposed. In literature [25], the regional energy management and optimized operating strategies of EVs and battery swapping station (BSS) are proposed according to the effects of the utility grid caused by uncoordinated charging of EVs and BSS. Literature [26] developed a management method considering load demand for electric vehicle charging. Literature [27] proposed a novel model of EV intelligent integrated station (IIS) and a new method for optimal operation of IISs to offer efficient batteries charging and exchange. In literature [28], an EV charging station equipped with photovoltaic panels, fuel cell, and energy storage system was proposed and an algorithm for economic dispatch of the controllable resources in such a station was presented. Literature [29] proposed a game theoretic approach for optimal scheduling of parking-lot electric vehicle charging. Recent studies on EVs from distribution network level mainly analyzed the impacts of EVs on distribution network, and related optimal charging and discharging strategies are proposed to reduce these impacts, but the coordination with transmission network is not considered.

Recent research also noticed impacts of EVs on the transmission network. Literature [30,31] evaluated the impact of the coordinated integration of EVs and wind energy in power system and proposed a stochastic security constrained unit commitment (UC) model. The mobility of EVs in the grid and uncertainties imposed by EVs, renewable energy resources (RES) are considered. The effect of plug-in EVs on UC, without considering V2G, was studied in [32,33]. The results showed that the ordered charging behavior of massive EVs according to power system condition and users demand could not only fill the valley load, but also avoid the impact of the peak load on power system. Literature [34–36] introduced a UC model with V2G scheduling in constrained parking lots, and an effective optimization scheme by using binary and integer versions of PSO was proposed. Literature [37] improved the model of the UC with V2G, considering wind power, solar power and their uncertainties. By considering reliability, literature [38] presented a UC model with V2G, but the operation cost was relatively higher. Literature [39] studied the coordination between EVs aggregator and system operator for scheduling of EV charging and V2G services, and showed that the EVs penetration levels could be increased by the coordination over their charging schedule. A stochastic unit commitment model was described in [40] considering coordination of thermal units, EVs, wind power, and the spinning reserve services provided by EVs. Literature [41] proposed an assessment tool considering power generation, transmission and distribution to assess the impact of EVs' uncontrolled charging and OPF-based smart charging on overall power systems, but wind power and the mobility of EVs are not considered. Researches on EVs charging strategy on transmission network level mainly concentrate on the coordination of EVs and generators. The distribution network is equivalent to a single node in the transmission network, and the network constraints in distribution network and spatial distribution restraints of EVs are ignored.

Nowadays the hierarchical dispatch schemes for electric vehicles have attracted much attention. Based on AC power flow constraints, literature [42] proposed a UC model based bi-layer optimization method for charging and discharging scheduling of EVs, but the mobility of EVs and renewable energy were not considered. Literature [43] developed a hierarchical networked micro-simulation environment to characterize renewables and electric vehicle's effect on the grid's load-carrying capacity, reliability of unit commitment and planning, and boundaries of grid safety, etc. Literature [44] presented a layered decomposition approach that permitted a holistic solution to the storage, scheduling and pricing problems of Electric Vehicle Charging Stations. In the top layer, at a long time scale, the optimal pricing scheme was obtained with grid power price and renewable energy represented by their long-term averages. The middle layer determined the optimal amounts of energy to buy from the grid and to use for charging. At the bottom layer, the scheduling policy of EV charging was determined while satisfying the total battery consumption obtained at the middle layer. Literature [45] presented a double-layer smart charging management algorithm (SCMA) for electric vehicles. The objective of first level of SCMA was to control each transformer power demand, transformer capacity, charging station status and the shortest way to reach suitable charger. During the charging process, the second level of SCMA was used to provide cost-effective and reliable charging as well as less impact

on power grid. However, the scale of the proposed SCMA was only limited in distribution system.

In current literature, the charing/discharging management of EVs has focused solely either on transmission grid or distribution grid.

As shown in Fig. 1, especially in China, EVs are connected to the power system from distribution network while thermal generators and large-scale RES are generally in transmission network. In China, the power from large-scale RES integrated on the transmission network is typically transmitted to loads center with long distance transmission lines. Comparing to this large volume power, the small capacity, decentralized RES in distribution network can be ignored when EVs are dispatched with the thermal generating units to accommodate the large-scale RES from transmission network. So the RES at distribution level are not considered in this paper.

The main contribution of this paper is to propose a temporal and spatial domain based bi-layer optimization schedule for large-scale EVs on both transmission grid level and distribution grid level. Firstly, on the upper layer, a UC based optimization model is established to improve the economy of the whole system by coordinating EVs with thermal generators, basic load, and wind power at the transmission grid level. As a result, the charing/discharging loads of EVs are optimized in temporal domain. Secondly, on the lower layer, an OPF based optimization model is proposed to minimize the power losses of distribution grid by reasonable spatial allocating the total EVs loads to each node at the distribution grid level. Both temporal optimization in transmission grid level and spatial optimization in distribution grid level are considered for the charing/discharging loads of EVs, therefore the proposed bi-layer optimization schedule can obtain significant performance on both safety and economy for the whole power system. The impacts of electricity price profile, EVs penetration and EVs load location are also analyzed.

The rest of this paper is organized as follows. Section 2 introduces the structure of the proposed bi-layer optimization strategy. Sections 3 and 4 propose the upper layer optimization strategy and the lower layer optimization strategy, respectively. Simulations and analysis are in Section 5. Finally, conclusion is drawn in Section 6.

2. The structure of the bi-layer optimization strategy

The proposed bi-layer optimization strategy, shown in Fig. 2, consists of an upper layer optimization in transmission system and a lower layer optimization in distribution system.

On the transmission grid level, the upper layer time-domain optimization coordinates the charging and/or discharge schedule of EVs with thermal generators, basic load, and wind power. The charging and discharging behaviors of EVs are optimized from temporal dimension. On the distribution network level, the lower layer spatial-domain optimization solves optimal load location for EVs. It can figure out where EVs should be charged or discharged. The charging and discharging behaviors of EVs are optimized from spatial dimension.

The goal of the upper layer optimization is to coordinate generators, wind power, and EVs to reduce the operating costs of units, charging costs of users and wind power curtailment. Based on the price of charging and discharging, number of EVs, parameters of thermal units, forecast curve of wind power and daily load, a UC model is proposed to optimize the output power of thermal units, wind power curtailment and EVs charging and discharging profile in temporal dimension.

By optimizing the spatial distribution of EVs charging and discharging load, the lower layer optimization in distribution system could reduce the operation costs of distribution grid. Based on the power supply from the transmission system, daily load demand in the distribution network and the profile of EVs charging and discharging, an OPF model is proposed for the lower level optimization.

3. The upper layer optimization strategy based on UC

From a view of transmission system, the upper layer optimization dispatches thermal generating units and EVs to obtain better economic performance on power grid operation and wind power accommodation. Considering the problem of wind power uncertainty and fluctuation [46], a scenario-based day-ahead UC model is proposed in the upper layer to coordinate thermal units, EVs and wind power to minimize the cost while meet the load demand.

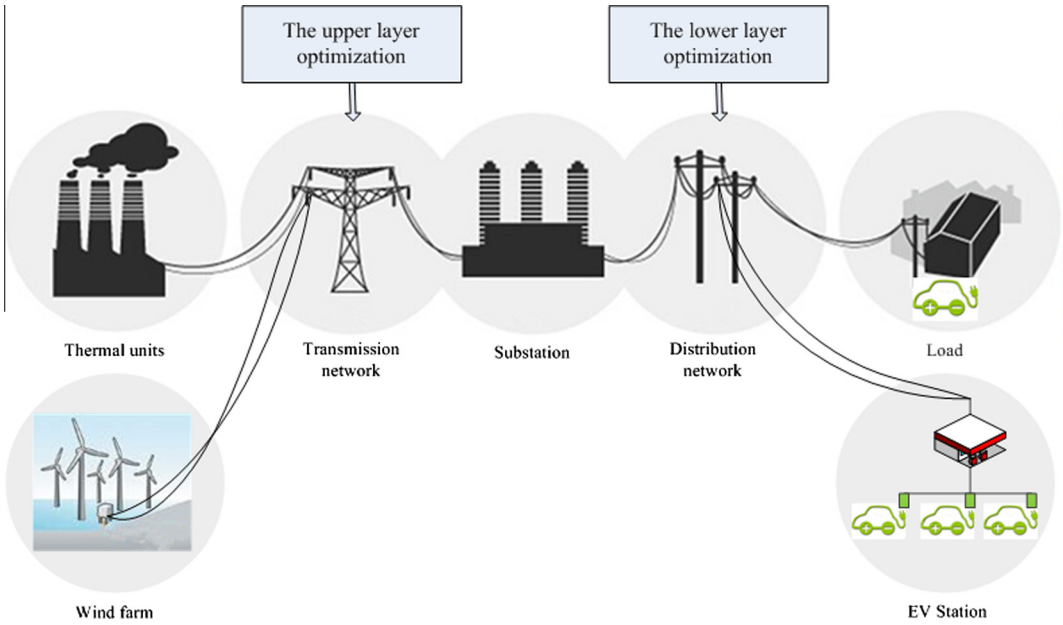

Fig. 1. The structure of power system.

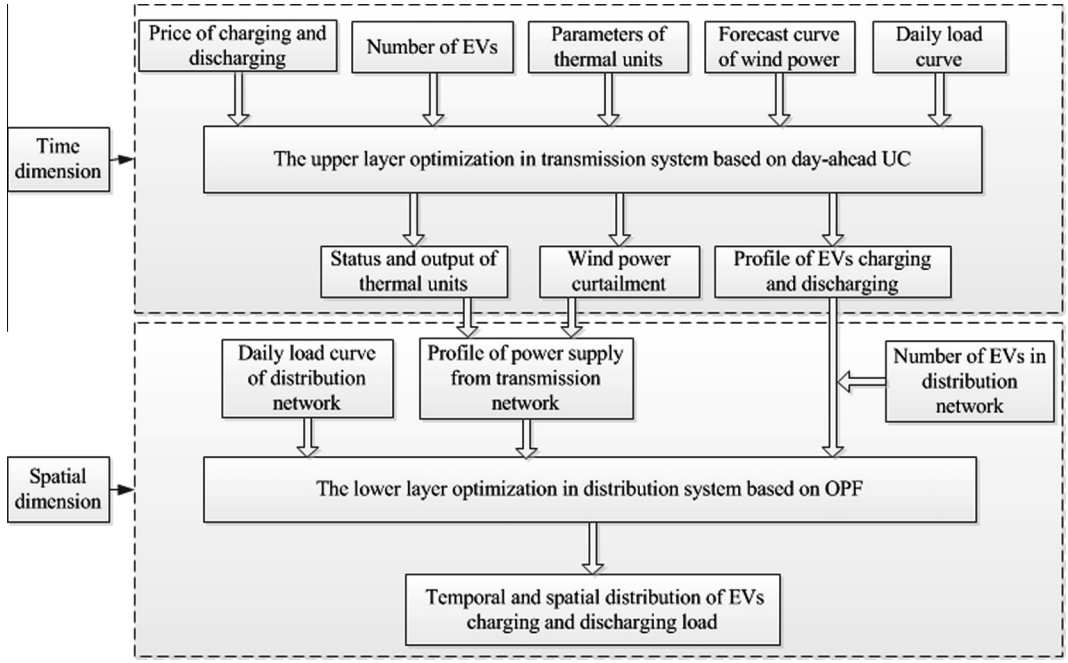

Fig. 2. The structure of the bi-layer optimization strategy.

The scenarios of wind power are generated based on Monte-Carlo simulation rather than thermal units. Different wind power profiles are generated independently according to [47] and contribute to different solutions of unit commitment. So the output of units is related to the scenarios of wind power. The scenarios are run independently.

3.1. The objective function

The objective function to reduce the operating costs of units, charging costs of users and wind power curtailment is described as follows:

3.1.1. Fuel cost

In power system, the fuel cost of a thermal unit is usually formulated as a quadratic function of its output as follow:

$$F_i(P^s_{i,t}) = a_i + b_i P^s_{i,t} + c_i P^{s2}_{i,t} \tag{1}$$

where a_i, b_i and c_i are positive fuel cost coefficients of unit i. $P^s_{i,t}$ is the output of unit i at time interval t in scenario s.

3.1.2. Emission

As part of the optimization objective, the PM2.5 emission of a thermal unit is calculated as a quadratic function of thermal unit's output [48]:

$$E_i(P^s_{i,t}) = Aar \cdot \omega \cdot (1 - \eta/100) \cdot (\alpha_i + \beta_i P^s_{i,t} + \gamma_i P^{s2}_{i,t})/10000 \tag{2}$$

where Aar is the average weight percentage of ash in the coal (%), and its default value is 20; ω is the conversion factor of total ash to PM2.5 (%) and its default value is 5.1; η is emission reduction efficiency (%) and its default value is 99 [48]. α_i, β_i, γ_i are coal consumption coefficients of unit i, and the emission of a unite is proportional to its coal consumption.

3.1.3. Start-up cost

The start-up cost for restarting an offline thermal unit is related to the temperature of the boiler. In this paper, a step function of the time-dependent start-up cost is as follows:

$$S_{i,t} = \begin{cases} S^h_i & \mathrm{T}^{off}_i < X^{off}_{i,t} \leqslant H^{off}_i \\ S^c_i & X^{off}_{i,t} > H^{off}_i \end{cases} \tag{3}$$

$$H^{off}_i = \mathrm{T}^{off}_i + \mathrm{T}^c_i \tag{4}$$

where H^{off}_i is the transition hour, S^h_i is the hot start cost of unit i, S^c_i is the cold start cost of unit i, $X^{off}_{i,t}$ is the continuously off-line time duration of unit i at time interval t, T^{off}_i is the minimal shut-down time of unit i, and T^c_i is the cold start time of unit i.

After linearization, it can be expressed as:

$$S_{i,t} \geqslant S^h_i (u_{i,t} - u_{i,t-1}), \quad \forall i \in N_g, \ \forall t \in T$$

$$S_{i,t} \geqslant S^c_i \left(u_{i,t} - \sum_{n=1}^{\mathrm{T}^{off}_i + \mathrm{T}^c_i + 1} u_{i,t-n} \right), \quad \forall i \in N_g, \ \forall t \in T$$

$$S_{i,t} \geqslant 0, \quad \forall i \in N_g, \ \forall t \in T$$

When $t - n$ is equal to zero, it refers to the initial state of unit. When $t - n$ is negative, it refers to the state of $n - t$ time intervals on the previous cycle.

3.1.4. Shut-down cost

Shut-down cost of a thermal unit is constant and the typical value is zero in standard systems [34].

3.1.5. Charging cost of users

The charging cost of users represents the financial cost of all EV users, calculated by charging cost minus discharging income:

$$U^s_t = \rho_{c,t} N^s_{c,t} P_c \Delta t - \rho_{d,t} N^s_{d,t} P_d \Delta t \tag{5}$$

where $\rho_{c,t}$ and $\rho_{d,t}$ are the electricity price of charging and discharging at time interval t, respectively. $N^s_{c,t}$ and $N^s_{d,t}$ are the number of EVs charging and discharging at time interval t in scenario s, respectively. P_c and P_d are the average charging and discharging power of EVs, respectively. Δt is the length of time interval, and it is one hour in this paper.

3.1.6. Wind curtailment cost

In order to improve the utilization of renewable energy, a penalty for wind power curtailment is considered in objective function:

$$W_t^s = \sum_{w=1}^{W} C_w \Delta P_{w,t}^s \tag{6}$$

where W is the total number of wind farms, C_w is the punish price of wind curtailment, and $\Delta P_{w,t}^s$ is the wind power curtailment of wind farm w at time interval t in scenario s.

Generally, a unit commitment plan is determined day-ahead and units' output will be adjusted according to different scenarios. Therefore our optimization target is to minimize the total start-up cost and expected operating cost of power system in different scenarios. Mathematically, considering thermal units, EV users, wind power and power grid, the objective function of the upper layer optimization is denoted as follows:

$$\min \sum_{t=1}^{T} \sum_{i=1}^{N_g} S_{i,t} u_{i,t}(1 - u_{i,t-1}) + E\left\{ \sum_{t=1}^{T} \left[\sum_{i=1}^{N_g} (F_i(P_{i,t}^s) + C_e E_i(P_{i,t}^s)) u_{i,t} + U_t^s + W_t^s \right] \right\} \tag{7}$$

where T is the total number of time intervals, N_g is the total number of thermal units. $E\{\cdot\}$ denotes the mathematical expectation of all scenarios. $u_{i,t}$ is the operation status of unit i at time interval t where 1 means online and 0 means offline. C_e is the punish price of PM2.5 emission. The probability of scenario s is $\Pr^s$. The calculation of the expectation can be presented as follows:

$$E(X) = X_1 * P(X_1) + X_2 * P(X_2) + \cdots + X_n * P(X_n)$$

where $P(X_n)$ is the probability of X_n.

3.2. Constraints

3.2.1. System power balance

Power system dispatch balances power supply with load demand. The power of all the committed units, EVs discharging and wind farms must be equal to the base load and EVs charging demand at any time:

$$\sum_{i=1}^{N_g} (u_{i,t} P_{i,t}^s) + P_d N_{d,t}^s + \sum_{w=1}^{W} (P_{w,t}^s - \Delta P_{w,t}^s) = D_t + P_c N_{c,t}^s, \quad \forall t \in T, \forall s \in S \tag{8}$$

where D_t is the base load demand at time interval t, $P_{w,t}^s$ is the predicted wind power of wind farm w at time interval t in scenario s.

3.2.2. Spinning reserve

To enhance system reliability, the adequate spinning reserves are represented as follows:

$$\sum_{i=1}^{N_g} (u_{i,t} P_i^{\max}) + P_d N_{d,t}^s + \sum_{w=1}^{W} (P_{w,t}^s - \Delta P_{w,t}^s) \geqslant D_t + P_c N_{c,t}^s + R_t, \quad \forall t \in T, \ \forall s \in S \tag{9}$$

where $P_i^{\max}$ is the maximum output of unit i and R_t is the system reserve requirement at time interval t.

3.2.3. Generation limits

Each unit has its output power range that is defined as:

$$P_i^{\min} u_{i,t} \leqslant P_{i,t}^s \leqslant P_i^{\max} u_{i,t}, \quad \forall i \in N_g, \ \forall t \in T, \ \forall s \in S \tag{10}$$

where $P_i^{\min}$ is the minimum output power of unit i.

3.2.4. Ramp rate

For each unit, the difference of output power in two adjacent time intervals is limited by ramp up/down rate. It can be represented as:

$$-R_{d,i} \leqslant P_{i,t}^s - P_{i,t-1}^s \leqslant R_{u,i}, \quad \forall i \in N_g, \ \forall t \in T, \ \forall s \in S \tag{11}$$

where $R_{u,i}$ and $R_{d,i}$ are ramp up and ramp down rate of unit i, respectively.

3.2.5. Minimum online/offline time

Once a unit is committed or uncommitted, it has to stay online or offline for a minimum time before switching to the other state again. The constraint of minimum online/offline time can be presented as follows:

$$(X_{i,t}^{on} - T_i^{on})(u_{i,t} - u_{i,t+1}) \geqslant 0, \quad \forall i \in N_g, \ \forall t \in T \tag{12}$$

$$(X_{i,t}^{off} - T_i^{off})(u_{i,t+1} - u_{it}) \geqslant 0, \quad \forall i \in N_g, \ \forall t \in T \tag{13}$$

where $X_{i,t}^{on}$ and $X_{i,t}^{off}$ are the time duration when unit i stays continuously online and offline at time interval t, respectively. T_i^{on} and T_i^{off} are the minimum online and offline time of unit i, respectively.

3.2.6. The number of EVs

At each time interval, the number of available EVs for charging or discharging is limited by:

$$N_{c,t}^s \leqslant N_{c,t}^{\max}, \quad \forall t \in T, \ \forall s \in S \tag{14}$$

$$N_{d,t}^s \leqslant N_{d,t}^{\max}, \quad \forall t \in T, \ \forall s \in S \tag{15}$$

where $N_{c,t}^{\max}$ and $N_{d,t}^{\max}$ are the maximum number of available EVs for charging and discharging at time interval t, respectively.

3.2.7. Charging/discharging duration

EVs require sufficient time for charging, but the discharging time has to be restricted so that EVs can retain enough energy to meet the owner's traveling need in the future. The total EVs charging or discharging duration should be constrained:

$$\sum_{t=1}^{T} N_{c,t}^s \Delta t = N_c^{\max} \Delta t_c, \quad \forall s \in S \tag{16}$$

$$\sum_{t=1}^{T} N_{d,t}^s \Delta t = N_d^{\max} \Delta t_d, \quad \forall s \in S \tag{17}$$

where $N_c^{\max}$ and $N_d^{\max}$ are the total number of EVs available for charging and discharging, respectively. Δt_c and Δt_d are the average charging time and discharging time of EVs, respectively.

3.2.8. Wind power curtailment limits

The relationship between wind power curtailment and the forecasted wind power is formulated as follows:

$$0 \leqslant \Delta P_{w,t}^s \leqslant P_{w,t}^s, \quad \forall w \in W, \forall t \in T, \ \forall s \in S \tag{18}$$

where $P_{w,t}^s$ denotes the forecasted wind power.

The wind power scenarios are generated according to literature [47]. Mathematical model of forecasting errors of wind power is first built based on historical data. Then, a large number of scenarios of the forecasting error time series of wind power are generated from stochastic simulations. Wind power scenarios are obtained by adding the expected value and error from forecast. Finally, scenario reduction techniques are used to cut the generated scenarios to a certain number of scenarios.

By linearizing [49] the UC-based upper layer model, the optimization problem is transformed into a mixed integer linear

programming (MILP) which can be solved by the CPLEX solver in AIMMS [50]. The optimization results include the online or offline status of each unit, the output power of each unit, the wind power curtailment and the total number of EVs charging and discharging at each time interval.

4. The lower layer optimization strategy based on OPF model

The lower layer optimization basing on OPF is implemented in the distribution system. The slack bus of the distribution system is the low-voltage side of a step-down transformer, whose high-voltage side is a node connected to the transmission grid.

With the optimization results of $N^s_{c,t}$ and $N^s_{d,t}$ obtained from the upper layer, the objective of the lower layer optimization is to minimize the power losses of distribution grid by arranging EVs to charge and discharge in the optimal location of the distribution grid.

Considering the mobility of EVs, an urban area can be divided into three types of functional zones: residential zone, commercial zone, and office zone [51]. During the daytime, most of EVs are parked in the office zone. At night almost all the EVs are parked in the residential zone.

4.1. Objective function

Distribution system operators prefer to reduce the energy losses in transmission to lower the cost of the distribution grid operation. The corresponding objective function can be defined as follows:

$$f = \min E\left[\sum_{t=1}^{T} P^s_{Loss,t}\right] \tag{19}$$

where $E[\cdot]$ is the expected value of all scenarios, and $P^s_{Loss,t}$ is the total network losses of distribution network at time interval t. Scenarios are the same to the upper layer.

4.2. Constraints

4.2.1. Active and reactive power balance

The active and reactive power balance must be satisfied at each node according to Kirchoff's laws:

$$P^s_{G\alpha,t} + P_d N^s_{d\alpha,t} - P_{D\alpha,t} - P_c N^s_{c\alpha,t} - P^s_{T\alpha,t} = 0, \quad \forall\alpha \in K,\ \forall t \in T,\ \forall s \in S \tag{20}$$

$$Q^s_{G\alpha,t} - Q_{D\alpha,t} - Q^s_{T\alpha,t} = 0, \quad \forall\alpha \in K,\ \forall t \in T,\ \forall s \in S \tag{21}$$

where K is the set of all nodes except the slack node, $P^s_{G\alpha,t}$ and $Q^s_{G\alpha,t}$ are the active power source and reactive power source of node α at time interval t in scenario s, respectively. $P_{D\alpha,t}$ and $Q_{D\alpha,t}$ are the active and reactive power load of node α at time interval t in scenario s, respectively. $N^s_{c\alpha,t}$ and $N^s_{d\alpha,t}$ are the number of EVs charging and discharging in node α at time interval t in scenario s, respectively. $P^s_{T\alpha,t}$ and $Q^s_{T\alpha,t}$ are the transmitted active and reactive power of node α at time interval t in scenario s, respectively:

$$P^s_{T\alpha,t} = V^s_{\alpha,t}\sum_{j\in\alpha} V^s_{j,t}(G_{\alpha j}\cos\theta^s_{\alpha j,t} + B_{\alpha j}\sin\theta^s_{\alpha j,t}) \tag{22}$$

$$Q^s_{T\alpha,t} = V^s_{\alpha,t}\sum_{j\in\alpha} V^s_{j,t}(G_{\alpha j}\sin\theta^s_{\alpha j,t} - B_{\alpha j}\cos\theta^s_{\alpha j,t}) \tag{23}$$

where $V^s_{\alpha,t}$ and $V^s_{j,t}$ are the voltage of node α and j at time interval t in scenario s, respectively; $G_{\alpha j}$ and $B_{\alpha j}$ are the real and imaginary part of admittance matrix, respectively; $\theta^s_{\alpha j,t}$ is the phase angle difference between node α and j at time interval t in scenario s.

4.2.2. Node voltage constraints

In order to ensure power quality and grid security, upper and lower limits of node voltage can be denoted as follows:

$$V_{\alpha,\min} \leqslant V^s_{\alpha,t} \leqslant V_{\alpha,\max}, \quad \forall\alpha \in K,\ \forall t \in T,\ \forall s \in S \tag{24}$$

where $V_{\alpha,\max}$ and $V_{\alpha,\min}$ are the upper and lower limits of node voltage, respectively.

4.2.3. Line capacity constraints

Transmission capacity of lines is limited by:

$$|P^s_{\alpha j,t}| \leqslant P_{\alpha j,\max}, \quad \forall\alpha, j \in K,\ \forall t \in T,\ \forall s \in S \tag{25}$$

where $P_{\alpha j,\max}$ is the maximal transmission capacity of line $\alpha - j$; $P^s_{\alpha j,t}$ is the power flow on transmission line $\alpha - j$ at time interval t in scenario s:

$$|P^s_{\alpha j,t}| = |V^s_{\alpha,t}V^s_{j,t}(G_{\alpha j}\cos\theta^s_{\alpha j,t} + B_{\alpha j}\sin\theta^s_{\alpha j,t}) - V^{s2}_{\alpha,t}G_{\alpha j}| \tag{26}$$

4.2.4. Constraints of charging piles in the nodes

There is a certain amount of charging piles in each node and so the maximal number of EVs connected to the grid is limited by:

$$0 \leqslant N^s_{c\alpha,t}, N^s_{d\alpha,t} \leqslant N_{\alpha,\max}, \quad \forall\alpha \in K,\ \forall t \in T,\ \forall s \in S \tag{27}$$

where $N_{\alpha,\max}$ is the number of charging piles in node α.

4.2.5. Number of EVs in the zone

The number of EVs in each zone is changing due to their mobility. The number of EVs available for charging and discharging in a certain zone can be formulated as:

$$\sum_{\alpha\in i} N^s_{c\alpha,t} = N^s_{ci,t}, i = \text{resid, comme, office}, \quad \forall t \in T,\ \forall s \in S \tag{28}$$

$$\sum_{\alpha\in i} N^s_{d\alpha,t} = N^s_{di,t}, i = \text{resid, comme, office}, \quad \forall t \in T,\ \forall s \in S \tag{29}$$

where $N^s_{ci,t}$ and $N^s_{di,t}$ are the number of EVs available for charging and discharging in zone i at time interval t in scenario s, respectively.

4.2.6. Availability of EVs

The total number of EVs available for charging and discharging in different zones is determined by the plan obtained from the upper layer schedule, and should satisfy:

$$\sum_{i\in I} N^s_{ci,t} = N^s_{c,t}, \quad \forall t \in T,\ \forall s \in S \tag{30}$$

$$\sum_{i\in I} N^s_{di,t} = N^s_{d,t}, \quad \forall t \in T,\ \forall s \in S \tag{31}$$

where I denotes all the zones.

The lower optimization model can be solved by a GMP-AOA solver of AIMMS. The optimization results are the number of EVs charging and discharging on each node in distribution grid at each time interval.

5. Case studies

A synthetic system consisting of both transmission and distribution grids is built to illustrate the effectiveness of the proposed bi-layer optimization strategy for EVs charging and discharging schedule. As shown in Fig. 3, a 10-unit transmission system including an 110 MW wind farm and an IEEE 33-bus distribution network is used to simulate the distribution grid. Node 0 in IEEE 33-bus system is a slack bus on the low-voltage side of a transformer, whose high-voltage side is a node of the 10-unit transmission grid. From the view of transmission system, distribution networks can be

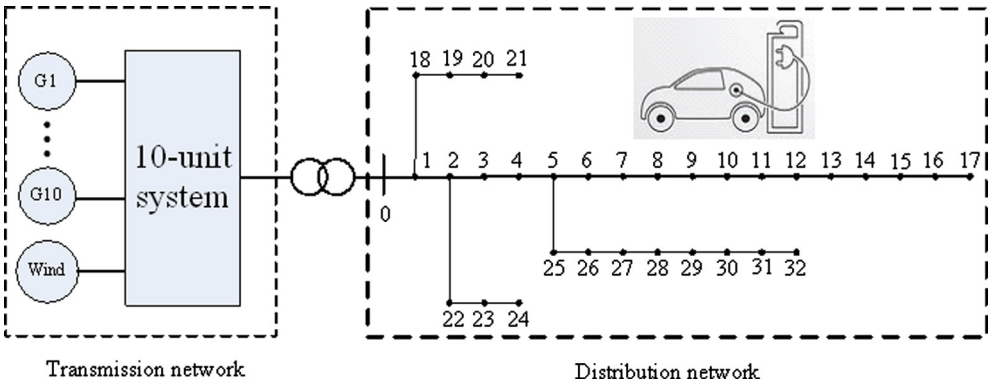

Fig. 3. The structure of power system including a transmission grid and a distribution grid.

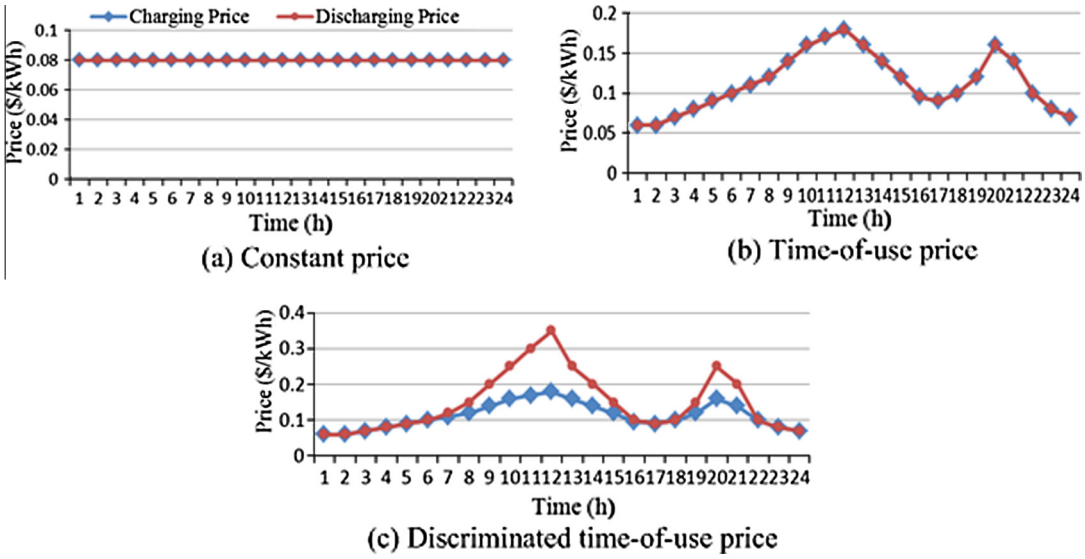

Fig. 4. The price profiles of charging and discharging.

taken as an equivalent load node. All the calculations have been carried out on a computer of Intel(R) Core(TM) i5-2500 3.3 GHz CPU, 3.42 GB RAM, Microsoft Windows XP OS and AIMMS optimization. The whole optimization calculation time is about half an hour.

5.1. Transmission system

Load demand and unit characteristics of the 10-unit system are obtained from [52]. The ramp rate of units can be referenced in [53]. Assume that the start-up ramp and shut-down ramp are equal to the minimum output of the unit, and the start-up time and shut-down time are both 1 h [54]. Coal consumption coefficients of units are collected from [55]. Scenarios of wind power and their probability data are collected from [47], and the outputs of wind power are multiplied by the proportional coefficient (0.2) to match the total installed capacity. The spinning reserve requirement is assumed to be 10% of the load demand, and the total schedule period is 24 h.

The prediction of EVs charging or discharging load is always a difficult problem. In our model, the boundary of EVs charging or discharging load can be obtained from historical data. Since we don't have enough historical data now, some reasonable assumptions can be used to evaluate the boundary of EVs load. The boundary of EVs charging load is determined by the number of EVs, charging power, the starting time of charging and the duration of charging. And the boundary of EVs discharging load is similar. In this paper, we make some reasonable assumptions about these parameters. The total number of EVs in the area covered by transmission system network is 150,000, and all EVs can participate in charging and discharging. The average charging time and discharging time of EVs are 6 h and 3 h, respectively. Both the average charging and discharging power of EVs are 1.8 kW. The charging and discharging frequency are both once per day. The maximum number of EVs available for charging and discharging is assumed to be constant at different time intervals. In this paper, our research focuses mainly on slow charging mode in which most users start to charge their EVs after back to home from work. Therefore, the uncertainty of EVs charging is relatively small. So, considering the uncertainty of EVs, the percentage of EVs available for charging ($N_{c,t}^{\max}$) and discharging ($N_{d,t}^{\max}$) at each time interval are set as 95% and 40%, respectively. The punish price of PM2.5 emission C_e is 3000 $/ton. The punish price of wind curtailment C_w is 100 $/MW h.

To estimate the impact of different electricity price profiles and different penetrations of EVs on the upper layer optimization, six cases are investigated in the upper layer optimization program. The price profiles of charging and discharging are shown in Fig. 4:

Case 1: There are no EVs considered in the optimization.

Table 1
The value of objective function in different cases.

	Objective function ($)	Fuel cost ($)	Emission (tons)	Start-up cost ($)	Power system operating cost ($)	Charging cost ($)	Wind curtailment (MW)
Case 1	541333.4	521542.4	5.320133	3830	541333.4	0	0
Case 2	611202.1	525665.3	5.415462	4490	546401.7	64800.4	0
Case 3	539010.3	530573.3	5.454205	4140	551075.9	−12065.6	0
Case 4	461360.2	530573.3	5.454205	4140	551075.9	−89715.7	0
Case 5	485745.3	525346.3	5.388713	3600	545112.4	−59367.1	0
Case 6	514623.5	524403.3	5.381615	4090	544638.1	−30014.6	0

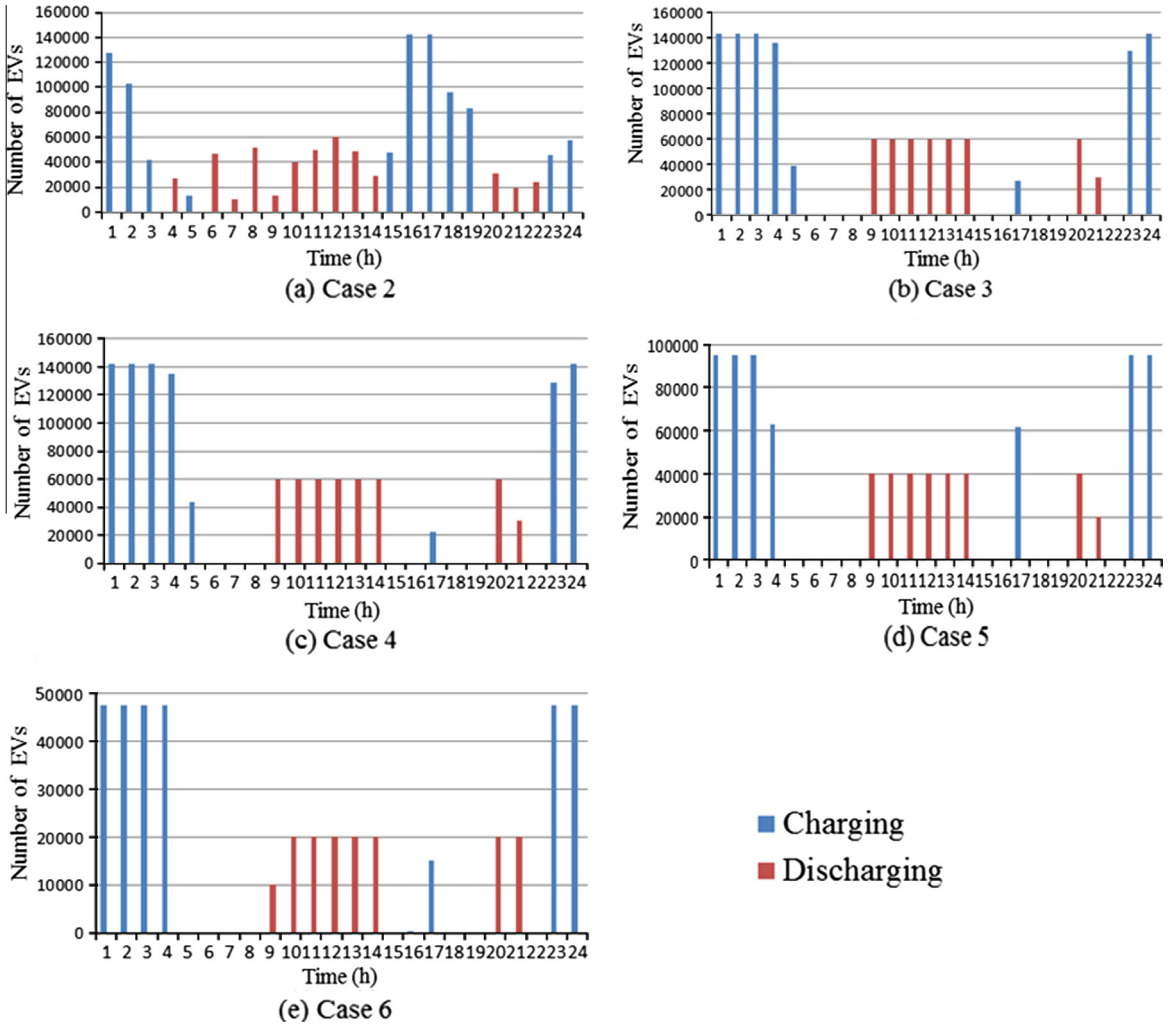

Fig. 5. The schedule of charging and discharging of different cases in scenario 1.

Case 2: There are 150,000 EVs in the system where the prices of charging and discharging are the same constant value in a day. The price profiles of charging and discharging in this case are shown in Fig. 4(a).
Case 3: There are 150,000 EVs in the system with the same price of charging and discharging that will fluctuate when load changes. The price profiles of charging and discharging in this case are shown in Fig. 4(b).
Case 4: There are 150,000 EVs in the system, and the charging prices are the same as Case 3. The discharging price is higher than the charging price in the period of heavy load, so it is more attractive to EVs to discharge. The price profiles of charging and discharging are shown in Fig. 4(c).
Case 5: There are 100,000 EVs in the system, and the price profiles are the same as Case 4.
Case 6: There are 50,000 EVs in the system, and the price profiles are the same as Case 4.

The expectations of the objective function, fuel cost, PM2.5 emissions, start-up cost, charging cost of users, and related wind curtailment over 20 wind power scenarios for six cases are shown in Table 1. A negative charging cost of users indicates they are earning by discharging power to the grid. From Table 1, it can be observed that the value of the objective function is decreasing from case 2 to case 4. Meanwhile, the benefit for the EV users is increasing, which represents with the increased number of EVs, the value of the objective function could also be decreased.

Since the total capacity of wind power is small comparing to the total capacity of thermal units, the wind curtailment is 0 MW in all

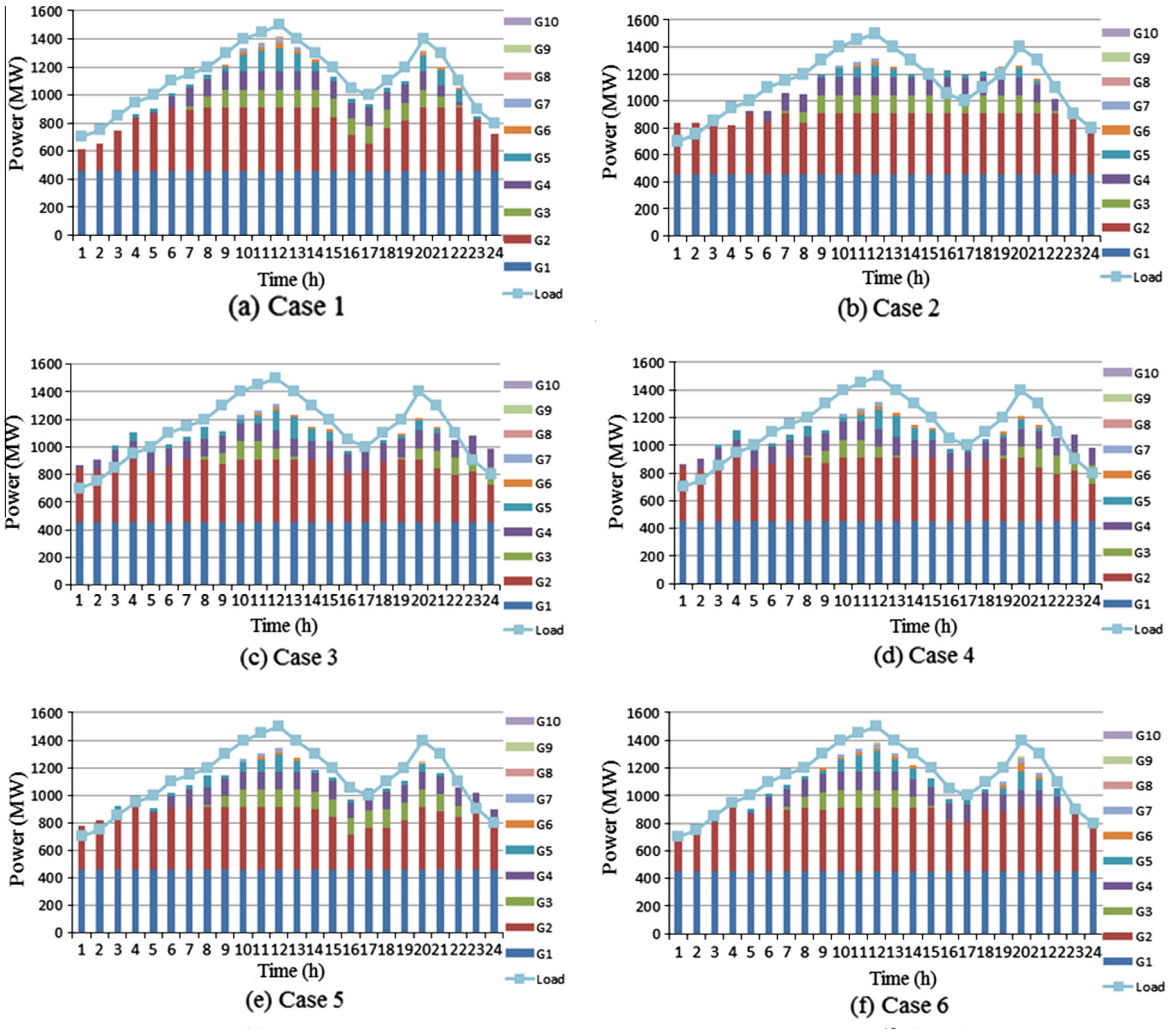

Fig. 6. The unit commitment results of different cases in scenario 1.

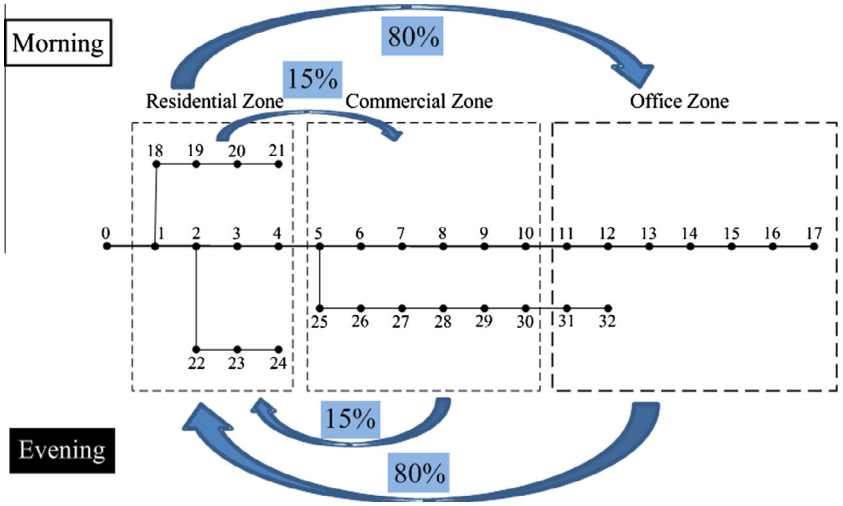

Fig. 7. The mobility of EVs in the network.

cases, which means 100% of wind power can be accommodated by the power system.

According to scenario 1, the schedule results of EVs' charging and discharging are shown in Fig. 5. The results of UC in different

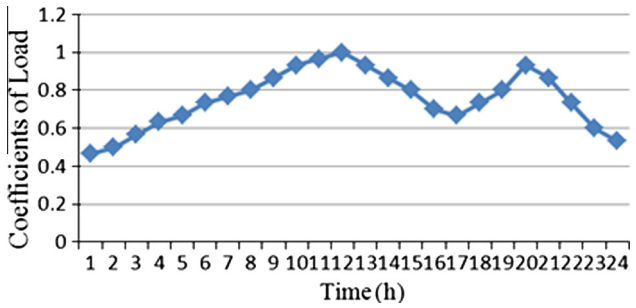

Fig. 8. The base load curve coefficients.

cases are shown in Fig. 6, where the difference between the load curve and the total output of units includes the accommodated wind power and EVs load.

The impacts of different price profiles on EVs schedule are compared among case 2, case 3 and case 4. In case 2, EVs charge and discharge with the same price, so the cost of all users will not vary during a day. As a result, the optimal objective is determined only by the interests of power system operating. However, in case 3 and case 4, users prefer to charge at lower price and discharge at higher price to obtain extra income, so the charging load mainly concentrates at night and the discharging load concentrates during heavy load periods. Case 2 has the lowest operating cost, but EVs total charging load peaks during 15:00–19:00 and EVs discharging load is concentrated during 6:00–9:00. In practice, it is difficult to schedule EVs charging and discharging in the commuting time periods. In contrast, users will not charge EVs with high price during the heavy load periods in case 3 and case 4, where the charging price profiles are the same. EV users prefer discharging in case 4 to discharging in case 3 because of higher discharging price, so that the objective value of case 4 is much smaller. The price profiles

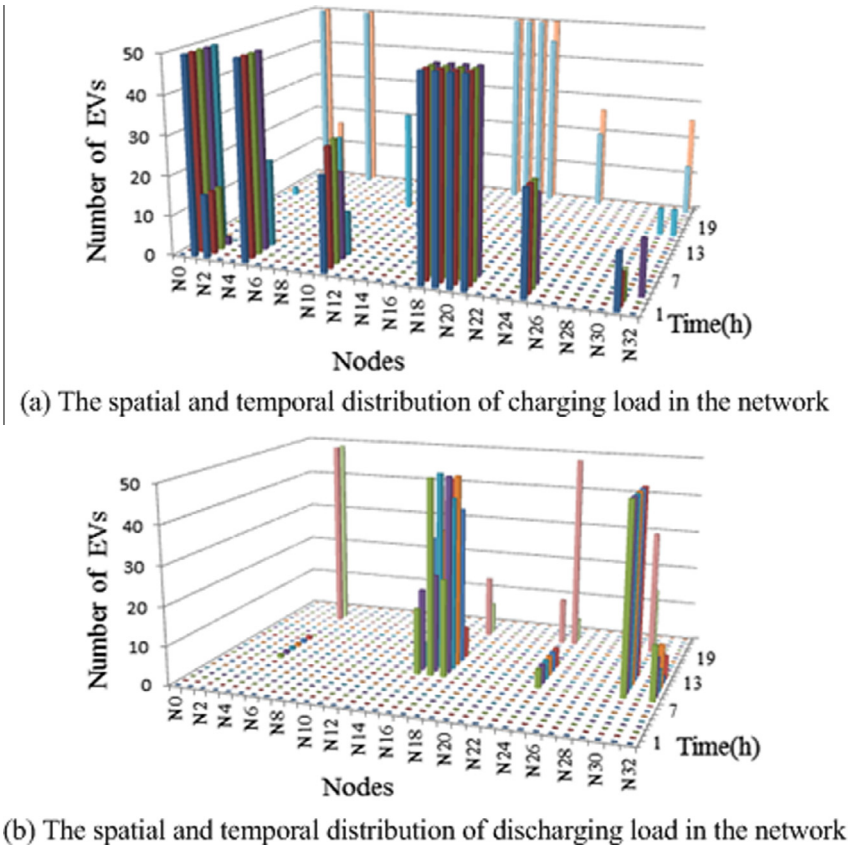

Fig. 9. The result of EVs charging and discharging schedule of case 8.

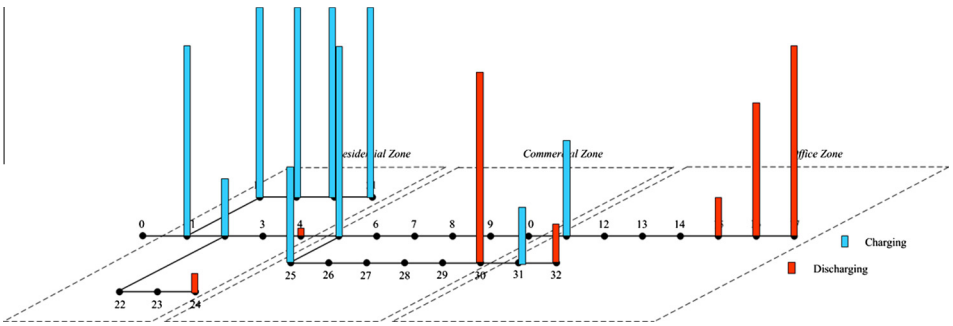

Fig. 10. The EVs charging and discharging load in the distribution network of case 8.

of case 4 are more efficient and practical, and the subsequent simulations in this paper are based on the price profiles of case 4.

Comparing with case 2, the charging load (15:00–19:00) in case 3 is much smaller due to the fluctuating price profile. So unit 3 is online from 7:00 to 22:00 to provide more power to EVs in case 2, while it is offline during 14:00 to 18:00 in case 3. Instead, unit 4 is online all the day in case 3 to satisfy the charging load which is shifted to night. The UC solution in case 3 and case 4 are the same despite the difference of price between charging and discharging.

The impacts of different EV penetrations on UC are compared among case 1, case 4, case 5 and case 6. As shown in Table 1, the power system operating costs increase with the increasing penetration of EVs due to providing more power to EVs. The output curve of total units becomes smoother that means the valley-to-peak is compensated by more price-shifted EVs load.

The results of other 19 scenarios are similar to scenario 1, so they are not considered in this paper.

5.2. Distribution grid simulation

The lower layer optimization is simulated in IEEE33-bus distribution system shown in Fig. 7. In this distribution system, the base power is 100 MVA and base voltage is 12.66 kV. The parameters of lines and the maximum load of nodes can be found in [56,57]. The base load curve coefficients shown in Fig. 8 are the same as the transmission system. The total number of EVs in this distribution grid is 400 determined by the ratio of the total distribution grid

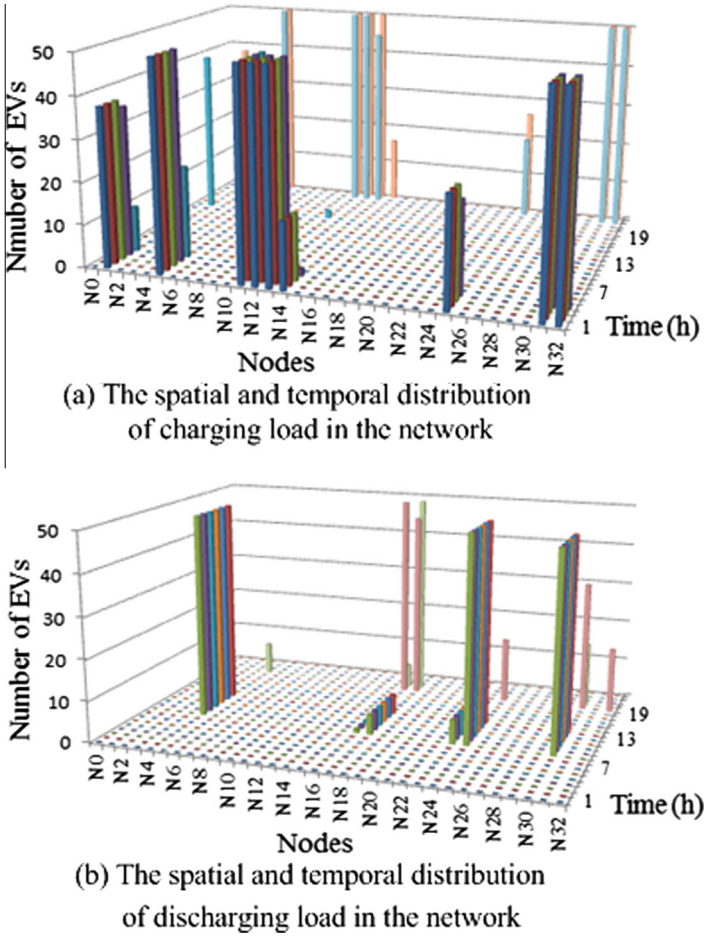

Fig. 11. The result of EVs charging and discharging schedule of case 9.

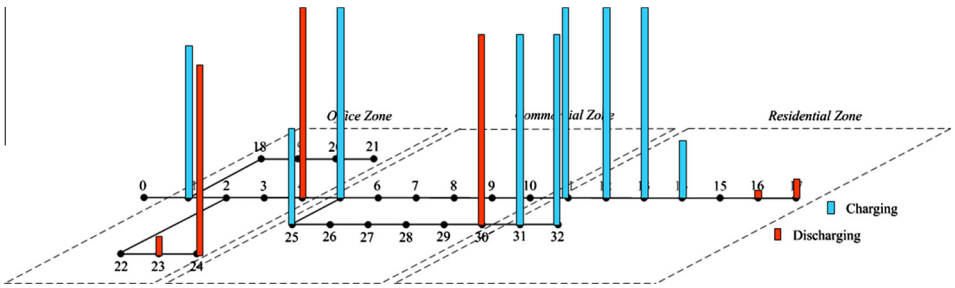

Fig. 12. The EVs charging and discharging load in the distribution network of case 9.

load to the total transmission grid load. And the maximum EV accommodation of each node is 50. In the initial state, there are 70% of EVs in residential zone, 20% of EVs in commercial zone, and 10% of EVs in office zone. During the daytime, most EVs are parked in office zone. As shown in Fig. 7, to describe the impact of the mobility characteristic of EVs on the distribution grid, we assume that 80% of EVs in residential zone will move to office zone and 15% will move to commercial zone in the morning, and these EVs will go back to residential zone in the evening. In this paper, EVs' driving characteristics and SOC are not considered. The percentage of EVs available for charging and discharging at each time interval are set to 0.95 and 0.4 respectively without considering EVs' driving characteristics and SOC.

We only select scenario 1 here to demonstrate the simulation results. The other scenario could be calculated the same way as scenario 1.

Three cases are studied in this section as follows:

Case 7: The simulation condition is the same as in case 1 with no EVs considered.

Case 8: The simulation condition is the same to case 4, and the information of three zones is shown in Fig. 7.

Case 9: To analyze the impact of EVs load location, the residential zone is swapped with the office zone, which means most of EVs are parked far from the slack bus at night. However, most of them move towards the slack bus in the daytime. The other simulation conditions are the same to case 8.

For case 8, the result of charging and discharging schedule is shown in Fig. 9, and the spatial distribution of EVs charging and discharging load in the network is shown in Fig. 10. We can see that the charging load mainly concentrates in node 1, 2, 5, 11, 18, 19, 20, 21, 26, 31 and 32. The discharging load mainly concentrates in node 4, 15, 16, 17, 24, 30 and 32. As the distribution network is typically a radial network, the power flows from the source to the end, and most power supply is provided from the slack bus which is an equivalent node of the transmission network. Therefore the EVs charging load is scheduled to be close to the slack bus to reduce network losses, and the EVs discharging load is scheduled to be close to the end nodes (i.e. node 17, 32) for the same reason. The temporal distribution of EVs load is the same to that of the transmission network.

For case 9, the result of charging and discharging schedule is shown in Fig. 11, and the spatial distribution of EVs charging and discharging load in the network is shown in Fig. 12. Comparing with case 8, we can draw the similar conclusions, namely, the EVs charging load is scheduled to be close to the slack bus and the EVs discharging load is scheduled to be close to the end nodes.

Fig. 13 shows the voltage distribution of the distribution network. It can be observed that the voltage decreases from the slack

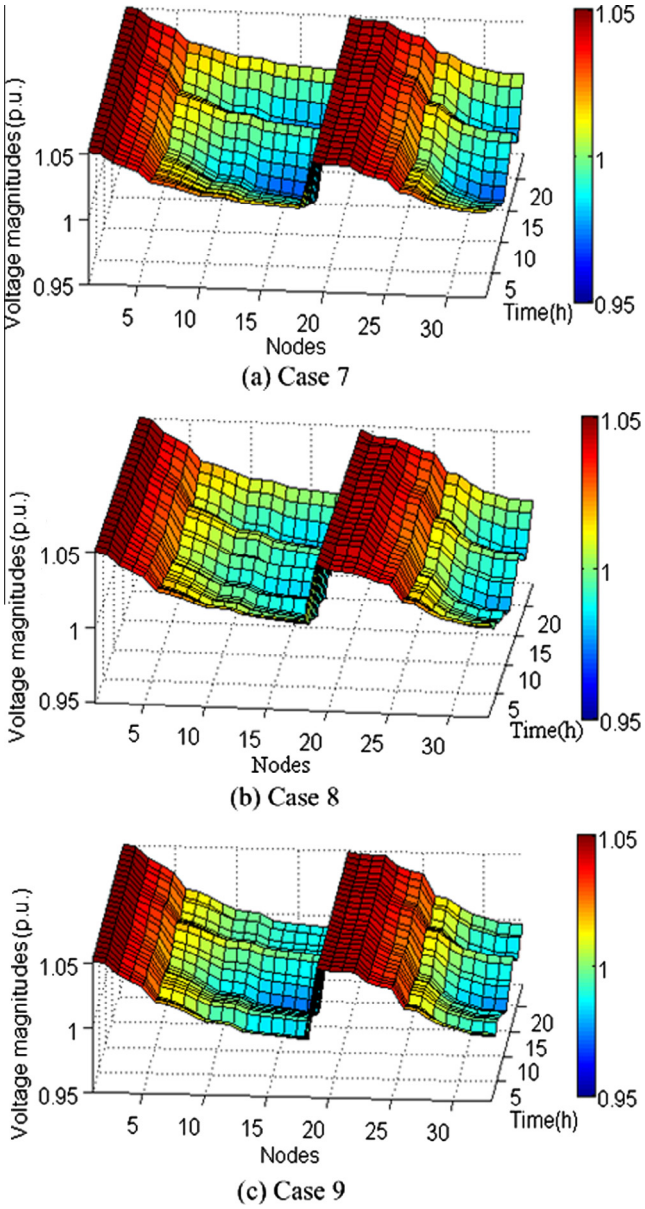

Fig. 13. The voltage distribution of the distribution network.

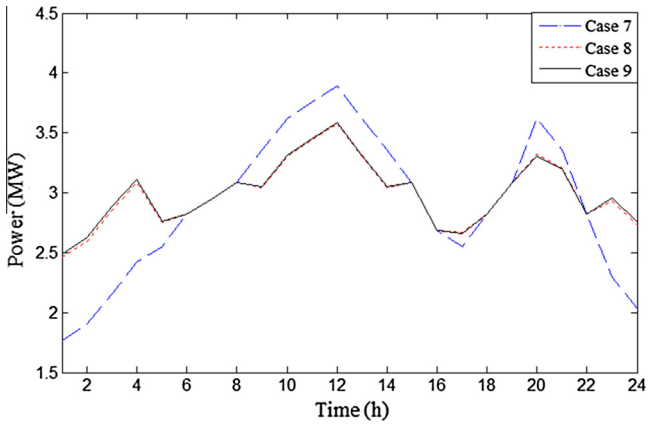

Fig. 14. The load curve of the slack bus (node 0) of the distribution network.

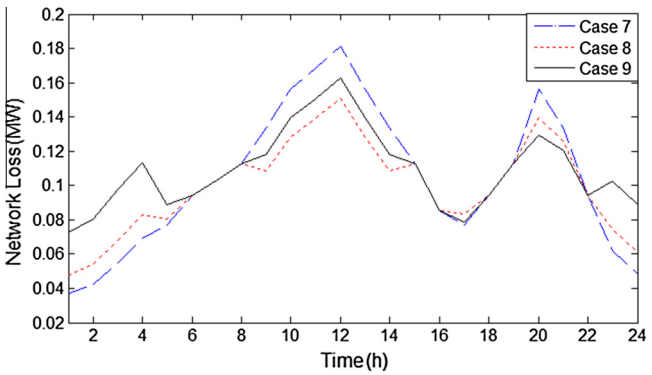

Fig. 15. The network loss curve of the distribution network.

bus to the end nodes. Comparing with case 7, EVs can improve the voltage level of the end nodes in both case 8 and case 9. Because more EVs are discharging in the end nodes during heavy load periods, case 8 yields better performance on the voltage level of end nodes than case 9.

The load curve of the slack bus (node 0) is shown in Fig. 14. The optimal schedule of EVs charging and discharging can shave the peak and fill the valley of load profiles. Because the load curve adjustment is only related to the total EVs load, it will not be affected by the location of EVs charging and discharging load.

The network loss of the distribution network is shown in Fig. 15. The network loss increases when EVs are charging, and it decreases when EVs are discharging. As EVs nighttime charging load in case 8 is closer to the slack bus than that in case 9, the network loss in case 8 is smaller than case 9 during 10:00 pm to 06:00 am. However, it is the opposite during 4:00 pm to 6:00 pm because most of the EVs are charging in the office zone in case 8. As EVs daytime discharging load in case 8 is closer to the end nodes than case 9, the network loss in case 8 is smaller than case 9 during 8:00 am to 3:00 pm. It is also the opposite during 7:00 pm to 10:00 pm because most of the EVs are discharging in the residential zone in case 8.

The total network loss of case 7, case 8 and case 9 are 2.4964 MW, 2.3898 MW and 2.6108 MW, respectively. Case 8 has smaller total network loss than case 9, because the voltage difference between slack bus and end nodes is smaller as a result of EVs charging load near the slack and discharging load near the end nodes.

In summary, installing the step-down substation of distribution network in residential zones and installing the end nodes of distribution network in office zones can achieve better economic performance on distribution network planning.

6. Conclusions

In this paper, a novel approach based on bi-layer optimization for scheduling EVs charging and discharging at both transmission grid level and distribution grid level is proposed to accommodate wind power and improve the economics of grid operation. The proposed strategy solves the scheduling problem of EVs charging and discharging load from temporal dimension and spatial dimension, respectively. The upper layer optimization in transmission grid coordinates EVs with thermal generators, base load, with consideration of wind power, to optimize load periods of EVs in the time domain. To achieve the solution given by the upper layer, the lower layer optimization in distribution grid level is trying to schedule the spatial location of EVs load. Through the coordination of the two-layer optimizations, the dispatcher of power grid can optimally allocate EVs charging and discharging load temporally and spatially. Also, the uncertainty and volatility of wind power are addressed in the proposed model by generating different wind power scenarios. To investigate the performance of the proposed bi-layer optimization strategy, simulations of different scenarios are carried out in a benchmark power system consisting of a 10-unit transmission grid and an IEEE 33-bus distribution grid. The impacts of electricity price profile, EVs penetration and EVs load location are also analyzed. Some conclusions are drawn as follows:

(1) By scheduling EVs charging and discharging temporally and spatially, the proposed bi-layer optimization strategy can accommodate wind power and improve the economics of grid operation and benefits of EV users.
(2) To optimally schedule EVs load, time-of-use price profile is necessary and higher discharging price profiles (e.g. profile c) is more effective and practical.
(3) The power system operating costs increase with the penetration of EVs, and the output curve of total units becomes smoother with more price-shifted EVs loads.
(4) In order to reduce the network loss and improve the voltage level of end nodes of the distribution network, the EVs charging load should be scheduled close to the step-down substation and the EVs discharging load should be scheduled close to the end nodes.
(5) The optimal schedule of EVs charging and discharging can shave the peak and fill the valley of load profiles, and it will not be affected by the location of EVs charging and discharging load.
(6) Installing the step-down substation of distribution network in residential zones and the end nodes of distribution network in office zones could achieve better economic performance on distribution network planning.

In real applications, by using the upper layer optimization model, the transmission system operator (TSO) will make a day-ahead UC plan based on the prediction of wind power, the thermal units, the number of EVs in the area of the transmission system, and the base load demand. As a result, the output power of the thermal units, the wind power outputs and the charging/discharging loads of EVs in different time intervals can be obtained. According to the number of EVs in each distribution system, the TSO will allocate the charging/discharging loads of EVs proportionally to each distribution system. Based on the spatial distribution of EVs and charging devices in the certain distribution system, the Distribution System Operators (DSO) will assign the total charging/discharging loads of EVs obtained from TSO to each node in the distribution system by using the lower layer optimization model. Moreover, the charging prices formulated by DSO can be used to guide the related EV owners to charge in the corresponding nodes in the distribution system.

Comparing with the charging/discharging schemes either in transmission system level or in distribution system level, the proposed bi-layer strategy considers the optimization in both transmission system level and distribution system level. So the optimization results can satisfy the economic and safety objectives of the total power system including transmission system and distribution system. However, the bi-layer optimization strategy needs more calculation time because of the largely increased system variable number.

The photovoltaic systems, EVs' driving characteristics and SOC will be considered in our future work.

Acknowledgments

The work is funded by the National Science Foundation of China (51277135, 50707021), the Fundamental Research Funds for the Central Universities (2042015kf1004), Wuhan Power Supply Company and Hebei Power Technology Research Institute.

References

[1] Pieltain FX et al. Assessment of the impact of plug-in electric vehicles on distribution networks. IEEE Trans Power Syst 2011;26(1):206–13.
[2] Trovao JP, Pereirinhaand PG, Jorge HM. Analysis of operation modes for a neighborhood electric vehicle with power sources hybridization. In: 2010 IEEE Vehicle Power and Propulsion Conference (VPPC). Lille; 2010.
[3] Clement-Nyns K, Haesenand E, Driesen J. The impact of charging plug-in hybrid electric vehicles on a residential distribution grid. IEEE Trans Power Syst 2010;25(1):371–80.
[4] Sousa T et al. Day-ahead resource scheduling in smart grids considering Vehicle-to-Grid and network constraints. Appl Energy 2012;96 (August):183–93.

[5] Monteiro V, Goncalvesand H, Afonso JL. Impact of electric vehicles on power quality in a smart grid context. In: 2011 11th international conference on Electrical Power Quality and Utilisation (EPQU). 2011; Lisbon.
[6] Foley A et al. Impacts of electric vehicle charging under electricity market operations. Appl Energy 2013;101:93–102.
[7] Fernandes C, Fríasand P, Latorre JM. Impact of vehicle-to-grid on power system operation costs: the Spanish case study. Appl Energy 2012;96:194–202.
[8] Yang Zhile, Li Kang, Foley Aoife. Computational scheduling methods for integrating plug-in electric vehicles with power systems: a review. Renew Sustain Energy Rev 2015;51:396–416.
[9] Richardson Peter, Moran Michael, Taylor Jason, Maitra Arindam, Keane Andrew. Impact of electric vehicle charging on residential distribution networks: an Irish demonstration initiative. In: 22nd International conference on electricity distribution. Stockholm; 2013.
[10] Richardson P, Flynn D, Keane A. Optimal charging of electric vehicles in low-voltage distribution systems. IEEE Trans Power Syst 2012;27(1):268–79.
[11] Yang J, He L, Fu S. An improved PSO-based charging strategy of electric vehicles in electrical distribution grid. Appl Energy 2014;128:82–92.
[12] Sortomme E et al. Coordinated charging of plug-in hybrid electric vehicles to minimize distribution system losses. IEEE Trans Smart Grid 2011;2 (1):198–205.
[13] Honarmand M, Zakariazadeh A, Jadid S. Optimal scheduling of electric vehicles in an intelligent parking lot considering vehicle-to-grid concept and battery condition. Energy 2014;65:572–9.
[14] Jian L, Zheng Y, Xiao X, et al. Optimal scheduling for vehicle-to-grid operation with stochastic connection of plug-in electric vehicles to smart grid. Appl Energy 2015;146:150–61.
[15] Amirioun MH, Kazemi A. A new model based on optimal scheduling of combined energy exchange modes for aggregation of electric vehicles in a residential complex. Energy 2014;69:186–98.
[16] Mart K, Wilfried S. Smart charging of electric vehicles with photovoltaic power and vehicle-to-grid technology in a microgrid; a case study. Appl Energy 2015;152:20–30.
[17] Emre CK, Jason SM, Douglas B, et al. Estimating the benefits of electric vehicle smart charging at non-residential locations: a data-driven approach. Appl Energy 2015;155:515–25.
[18] O'Connell Alison, Flynn Damian, Richardson Peter, Keane Andrew. Controlled charging of electric vehicles in residential distribution networks. In: 2012 3rd IEEE PES Innovative Smart Grid Technologies Europe (ISGT Europe). Berlin; 2012.
[19] Richardson Peter, Flynn Damian, Keane Andrew. Local versus centralized charging strategies for electric vehicles in low voltage distribution systems. IEEE Trans Smart Grid 2012;3(2):1020–8.
[20] Sortomme Eric, El-Sharkawi Mohamed A. Optimal charging strategies for unidirectional vehicle-to-grid. IEEE Trans Smart Grid 2011;2(1):131–8.
[21] Sortomme E, Cheung KW. Intelligent dispatch of electric vehicles performing vehicle-to-grid regulation. In: IEEE international electric vehicle conference. Greenville; 2012.
[22] Sortomme Eric, El-Sharkawi Mohamed A. Optimal combined bidding of vehicle-to-grid ancillary services. IEEE Trans Smart Grid 2012;3(1):70–9.
[23] Al-Awami AT, Sortomme E. Electric vehicle charging modulation using voltage feedback control. In: IEEE power & energy society general meeting. Vancouver; 2013.
[24] Ansari Muhammad, Al-Awami Ali T, Sortomme Eric, Abido MA. Coordinated bidding of ancillary services for vehicle-to-grid using fuzzy optimization. IEEE Trans Smart Grid 2015;6(1):261–70.
[25] Zhang Mingrui, Chen Jie. The energy management and optimized operation of electric vehicles based on microgrid. IEEE Trans Delivery 2014;29(3):1427–35.
[26] Moon Sang-Keun, Kim Wook-Won, Sin Je-Seok, Na Mun-Su, Kim Jin-O. Evaluation of the charging effects of electric vehicles on power systems, taking into account optimal charging scenarios. In: IEEE power & energy society general meeting. Denver; 2015.
[27] Xie Da, Chu Haoxiang, Gu Chenghong, Li Furong, Zhang Yu. A novel dispatching control strategy for EVs intelligent integrated stations. IEEE Trans Smart Grid 2015:1–10.
[28] Liao Yung-Tang, Lu Chan-Nan. Dispatch of EV charging station energy resources for sustainable mobility. IEEE Trans Transp Electrification 2015;1 (1):86–93.
[29] Lei Zhang, Li Yaoyu. A game theoretic approach to optimal scheduling of parking-lot electric vehicle charging. IEEE Trans Veh Technol 2015:1–10.
[30] Khodayar ME, Leiand W, Shahidehpour M. Hourly coordination of electric vehicle operation and volatile wind power generation in SCUC. IEEE Trans Smart Grid 2012;3(3):1271–9.
[31] Khodayar ME, Leiand W, Zuyi L. Electric vehicle mobility in transmission-constrained hourly power generation scheduling. IEEE Trans Smart Grid 2013;4(2):779–88.
[32] Jing ZX, et al. Research on unit commitment in power system with electric vehicles classification. In: Power and energy society general meeting (PES), 2013 IEEE. Vancouver, BC; 2013.
[33] Lu L et al. Unit commitment in power systems with plug-in electric vehicles. Automat Electric Power Syst 2011;35(21):16–20.
[34] Saber A, Venayagamoorthy GK. Optimization of vehicle-to-grid scheduling in constrained parking lots. In: Power & energy society general meeting, 2009. PES '09. IEEE. Calgary, AB; 2009.
[35] Saber A, Venayagamoorthy GK. Unit commitment with vehicle-to-Grid using particle swarm optimization. In: PowerTech, 2009 IEEE Bucharest. Bucharest; 2009.
[36] Saber AY, Venayagamoorthy GK. Intelligent unit commitment with vehicle-to-grid — a cost-emission optimization. J Power Sources 2010;195(3):898–911.
[37] Saber A, Venayagamoorthy GK. Resource scheduling under uncertainty in a smart grid with renewables and plug-in vehicles. IEEE Syst J 2012;6(1):103–9.
[38] Ghanbarzadeh T, Goleijaniand S, Moghaddam MP. Reliability constrained unit commitment with electric vehicle to grid using Hybrid Particle Swarm Optimization and Ant Colony Optimization. In: Power and energy society general meeting, 2011 IEEE. San Diego, CA; 2011.
[39] Ortega-Vazquez MA, Bouffardand F, Silva V. Electric vehicle aggregator/system operator coordination for charging scheduling and services procurement. IEEE Trans Power Syst 2013;28(2):1806–15.
[40] Cong L et al. Assessment of impacts of PHEV charging patterns on wind-thermal scheduling by stochastic unit commitment. IEEE Trans Smart Grid 2012;3(2):675–83.
[41] Gonzalez Vaya M, et al. On the interdependence of intelligent charging approaches for plug-in electric vehicles in transmission and distribution networks. In: 2012 3rd IEEE PES international conference and exhibition on innovative smart grid technologies (ISGT Europe). Berlin; 2012.
[42] Cai Q et al. An SCUC-based optimization approach for power system dispatching with plug-in hybrid electric vehicles. Automat Electric Power Syst 2012;36(01):38–46.
[43] Chakraborty SV, Shukla SK, Thorp J. A hierarchical networked micro-simulator to study grid-integration of renewables and electric vehicles. In: 2013 Workshop on Modeling and Simulation of Cyber-Physical Energy Systems (MSCPES), IEEE; 2013. p. 1–6.
[44] Ma KL, Xie L, Kumar PR. A layered architecture for EV charging stations based on time scale decomposition. In: 2014 IEEE international conference on Smart Grid Communications (SmartGridComm). IEEE; 2014. p. 674–9.
[45] Yagcitekin B, Uzunoglu M. A double-layer smart charging strategy of electric vehicles taking routing and charge scheduling into account. Appl Energy 2016;167:407–19.
[46] Xi-Yuan M, Yuan-Zhangand S, Hua-Liang F. Scenario generation of wind power based on statistical uncertainty and variability. IEEE Trans Sust Energy 2013;4 (4):894–904.
[47] Yu L. Studies on unit commitment considering wind power based on scenario analysis in power systems. Jinan: Shandong University; 2013.
[48] Department of Sustainability, Environment, Water, Population and Communities of Australia. Emission estimation technique manual for fossil fuel electric power generation; 2012. <http://www.npi.gov.au/system/files/resources/d3fd3837-b931-e3e4-e105-98a9f7048ac6/files/elec-supply.pdf>.
[49] Carrio X, Nand M, Arroyo JM. A computationally efficient mixed-integer linear formulation for the thermal unit commitment problem. IEEE Trans Power Syst 2006;21(3):1371–8.
[50] The AIMMS Website; 2014. <http://www.aimms.com/>.
[51] Mu Y et al. A Spatial-Temporal model for grid impact analysis of plug-in electric vehicles. Appl Energy 2014;114:456–65.
[52] Kazarlis SA, Bakirtzisand A, Petridis V. A genetic algorithm solution to the unit commitment problem. IEEE Trans Power Syst 1996;11(1):83–92.
[53] Min Y. Research on power system unit commitment with pumped storage power plant and wind power. Shanghai: Shanghai Jiaotong University; 2013.
[54] Xiaoyu H. Unit commitment using an improved lagrangian relaxation method. Beijing: North China Electric Power University; 2010.
[55] Xueshan H, Zuo L. Optimal unit commitment considering unit's ramp-rate limits. Power Syst Technol 1994;18(06):11–6.
[56] Venkatesh B, Ranjanand R, Gooi HB. Optimal reconfiguration of radial distribution systems to maximize loadability. IEEE Trans Power Syst 2004;19 (1):260–6.
[57] Baran ME, Wu FF. Network reconfiguration in distribution systems for loss reduction and load balancing. IEEE Trans Power Delivery 1989;4(2):1401–7.